New Phytologist

Research

# Warming drives a 'hummockification' of microbial communities associated with decomposing mycorrhizal fungal necromass in peatlands

**François Maillard[1], Christopher W. Fernandez[1,2], Sunil Mundra[3,4], Katherine A. Heckman[5], Randall K. Kolka[6], Håvard Kauserud[3] and Peter G. Kennedy[1]**

[1]Department of Plant & Microbial Biology, University of Minnesota, St Paul, MN 55108, USA; [2]Department of Forestry, Michigan State University, East Lansing, MI 48824, USA; [3]Section for Genetics and Evolutionary Biology (EvoGene), Department of Biosciences, University of Oslo, Oslo NO-0316, Norway; [4]Department of Biology, College of Science, United Arab Emirates University, Al-Ain, Abu-Dhabi, UAE; [5]USDA Forest Service Northern Research Station, Houghton, MI 49931, USA; [6]USDA Forest Service Northern Research Station, Grand Rapids, MN 55744, USA

Author for correspondence:
*François Maillard*
*Email: francois.maillard2@gmail.com*

Received: *30 May 2021*
Accepted: *15 September 2021*

*New Phytologist* (2021)
**doi**: 10.1111/nph.17755

**Key words:** bog microtopography, climate change, decomposition, mycorrhizal residues, necromass congeneric colonization advantage, SPRUCE.

## Summary

- Dead fungal mycelium (necromass) represents a critical component of soil carbon (C) and nutrient cycles. Assessing how the microbial communities associated with decomposing fungal necromass change as global temperatures rise will help in determining how these belowground organic matter inputs contribute to ecosystem responses.
- In this study, we characterized the structure of bacterial and fungal communities associated with multiple types of decaying mycorrhizal fungal necromass incubated within mesh bags across a 9°C whole ecosystem temperature enhancement in a boreal peatland.
- We found major taxonomic and functional shifts in the microbial communities present on decaying mycorrhizal fungal necromass in response to warming. These changes were most pronounced in hollow microsites, which showed convergence towards the necromass-associated microbial communities present in unwarmed hummocks. We also observed a high colonization of ericoid mycorrhizal fungal necromass by fungi from the same genera as the necromass.
- These results indicate that microbial communities associated with mycorrhizal fungal necromass decomposition are likely to change significantly with future climate warming, which may have strong impacts on soil biogeochemical cycles in peatlands. Additionally, the high enrichment of congeneric fungal decomposers on ericoid mycorrhizal necromass may help to explain the increase in ericoid shrub dominance in warming peatlands.

## Introduction

Rising temperatures associated with elevated atmospheric greenhouse gas concentrations are dramatically affecting the composition and functioning of many ecological communities (Traill *et al.*, 2010; Reich *et al.*, 2015; Garcia *et al.*, 2018). This is particularly true in high-latitude ecosystems, where the effects of increased temperatures are occurring most rapidly (Serreze *et al.*, 2000; Ito *et al.*, 2020). Among the ecosystems of highest concern globally are peatlands (Belyea & Malmer, 2004; Bragazza *et al.*, 2013). Despite their relatively low land area coverage (estimated at 3% of the Earth's surface), peatlands currently act as major belowground carbon (C) sinks (estimated to contain 30% of Earth's soil C) as a result of repressed organic matter decomposition from the anoxic conditions associated with high water tables (Gorham, 1991). Increasing temperatures, however, are associated with increased evapotranspiration, declines in peatland water table depths (Bragazza *et al.*, 2013; Fernandez *et al.*, 2019) and greater organic matter decomposition (Moore & Dalva, 1993; Samson *et al.*, 2018). Collectively, these changes can shift peatland ecosystems from net C sinks to net C sources (Gallego-Sala *et al.*, 2018; Hanson *et al.*, 2019), which in turn drives greater warming.

A critical ecological feature of peatlands is a subtly undulating microtopography that consists of raised patches of *Sphagnum* mosses known as hummocks and depressed areas of *Sphagnum* known as hollows. Along with changes in *Sphagnum* species composition (Robroek *et al.*, 2007; Breeuwer *et al.*, 2009), peatland microbial communities have also been shown to differ with microtopography, with hummock communities containing aerobic chemoorganotrophic, methanotrophic and chemoheterotrophic bacteria as well as a high presence of moss-associated fungi and hollow communities containing anaerobic/facultative anaerobic chemoorganotrophic bacteria, nitrate-

reducing bacteria, methanogenic archaea and a higher presence of root-associated fungi (Asemaninejad *et al.*, 2017, 2019). Owing to their differential proximity to the water table and therefore aerobic conditions, decomposition of organic matter typically occurs faster in hummocks than in hollows (Moore & Basilenko, 2006; Moore *et al.*, 2007). However, as air temperatures rise, this pattern is likely to be modified, with warming increasing aerobic conditions in hollows and thereby stimulating greater rates of decomposition (Fernandez *et al.*, 2019).

Many high-latitude peatlands contain additional plant functional types along with *Sphagnum* mosses, including both ericaceous shrubs and trees. Both trees and shrubs host diverse root-associated fungal communities (Andersen *et al.*, 2013) and form ericoid mycorrhizal and ectomycorrhizal symbiosis, respectively, which play a well-recognized role in facilitating host plant acquisition of nutrients from organic sources (Read *et al.*, 2004). When mycorrhizal fungi die, their extensive mycelia, including recalcitrant cell wall components, such as melanin (Ryan *et al.*, 2020), contribute to the soil organic matter (SOM) pool. Given the much lower initial C : nitrogen (N) ratio of fungal necromass compared with *Sphagnum* mosses and other dead plant inputs (Wang *et al.*, 2015), this belowground organic matter input may be a particularly important source of N in peatlands and other ecosystems (Read *et al.*, 2004; Zhang *et al.*, 2019). Mycorrhizal fungi might also contribute directly to their host nutrition by mining nutrients and notably N, the soil fungal necromass pool. For example, N transfer from fungal necromass and derived compounds has been reported for both ericoid mycorrhizal and ectomycorrhizal fungi (Leake & Read, 1990; Kerley & Read, 1995; Akroume *et al.*, 2019). Internal recycling of mycelium (i.e. fungi decomposing their own dead mycelium) has also been suggested as a potential source of N for the host plant, particularly for the cord-forming ectomycorrhizal fungi in boreal forests (Clemmensen *et al.*, 2015), but mycorrhizal fungal necromass may also be exploited by closely related mycorrhizal taxa, which probably have enzymatic capacities well matched to modify compounds present in the mycelia of their congeners.

The recent application of high-throughput molecular identification methods has provided greater insight into the structure of microbial communities associated with decomposing fungal necromass. For example, it is now clear that fungal necromass is quickly decomposed by fast-growing bacteria and fungi, with significant changes in community composition towards taxa with stronger enzymatic capacities over time (Brabcová *et al.*, 2016; Maillard *et al.*, 2020, 2021). In temperate ecosystems, it has also been shown that some ectomycorrhizal fungi colonize fungal necromass efficiently, supporting the potential role of dead mycelium as a nutrient source for root-associated fungi (Brabcová *et al.*, 2016; Fernandez & Kennedy, 2018; Maillard *et al.*, 2021). However, in studies using mycorrhizal fungi as necromass, mycorrhizal fungal colonizers were not closely related to the species that produced the substrate (Brabcová *et al.*, 2016; Fernandez & Kennedy, 2018). There also appear to be important differences in the structure of decomposer microbial communities depending on the chemistry of the fungal necromass being colonized, particularly in relation to initial nitrogen and melanin content (Brabcová *et al.*, 2018; Fernandez & Kennedy, 2018; Beidler *et al.*, 2020). Relative to the effects of time and initial necromass chemistry, however, much less is known about the extent to which necromass-associated microbial community structure is influenced by extrinsic environmental factors (Fernandez *et al.*, 2016). Recent studies have found that necromass-associated microbial communities can differ along natural gradients of vegetation type (grassland vs forest (Beidler *et al.*, 2020), pine vs oak forest (Fernandez & Kennedy, 2018), and ectomycorrhizal-dominated vs arbuscular mycorrhizal-dominated forests (Beidler *et al.*, 2020)), but how these communities respond to experimentally altered climatic conditions is currently unknown.

The goal of this study was to determine how the microbial communities associated with decomposing mycorrhizal fungal necromass respond to changes in peatland temperatures under field conditions. To do so, we incubated necromass from mycorrhizal fungi with diverse initial chemistries in the SPRUCE experiment in northern Minnesota, USA. SPRUCE consists of a series of large open-topped chambers in which below- and aboveground heating is being applied in + 2.25°C increments up to 9°C above ambient temperatures (Hanson *et al.*, 2017). Our previous work in this system found that increased ecosystem temperatures stimulated the decomposition of mycorrhizal fungal necromass, but only in the hollow microsites, where water table depth was significantly lowered by the warming (Fernandez *et al.*, 2019). Here, we focus on three primary questions: to what extent do changes in microbial community structure on mycorrhizal fungal necromass track the observed patterns of mass loss in regard to a temperature by microtopography interaction; what chemical attributes of decomposed mycorrhizal fungal necromass most strongly correlate with shifts in microbial community structure; and is decomposing mycorrhizal fungal necromass a potential hotspot of colonization by mycorrhizal fungi?

## Materials and Methods

### Study site

The SPRUCE project is an ecosystem climate manipulation experiment located in a forested peatland at the Marcell Experimental Forest in northern Minnesota, USA (47°30.4760′N, 93°27.1620′W). The climate change treatments are located in the S1 bog, which is a weakly ombrotrophic peatland with a perched water table (Sebestyen *et al.*, 2011). The vegetation is codominated by *Picea mariana* and *Larix laricina* trees, with ericaceous shrubs such as *Rhododendron groenlandicum* and *Chamaedaphne calyculata*, and a thick bryophyte layer dominated by *Sphagnum angustifolium* and *S. fallax* in hollows and *S. magellanicum* on hummocks. The + 0, + 2.25, + 4.5, + 6.75 and + 9°C warming treatments are run in conjunction with elevated $CO_2$ treatment at +500 ppm above ambient reference plots (*c.* 900 ppm) in large open-top chambers (12 m in diameter). Further environmental and experimental details associated with SPRUCE are provided in Hanson *et al.* (2017).

### Necromass generation

Necromass was generated from four mycorrhizal fungal species that naturally associate with either ectomycorrhizal tree hosts or ericoid mycorrhizal shrubs in the S1 site: *Cenococcum geophilum* (ectomycorrhizal), *Suillus grisellus* (ectomycorrhizal), *Meliniomyces bicolor* (ectomycorrhizal and ericoid mycorrhizal) and *Oideodendron griseum* (ericoid mycorrhizal). (We are aware of recent taxonomic updates to the genus *Meliniomyces* (Hambleton & Sigler, 2005; Fehrer *et al.*, 2019), but because this name was applied in our previous work in this study system (Fernandez *et al.*, 2019) and there is still widespread usage of this genus name in the literature, we have maintained its application here.) Fungal isolates were grown in 50 ml of half-strength potato dextrose broth (PDB, Difco; BD Products, Franklin Lakes, NJ, USA) in 125 ml flasks shaken on orbital shakers at 80 rpm at room temperature for 30 d. Fungal biomass was then harvested, rinsed in deionized water, and dried at 27°C in a drying oven for 24 h. This temperature was chosen to minimize any chemical changes in dead mycelium that would be generated by drying at higher temperatures. Nylon mesh litter bags (*c.* 3 × 3 cm, 53 µm nylon mesh (Elko, Minneapolis, MN, USA)) containing on average 42 mg dry mass of the four necromass types were heat-sealed (American International Electric Inc., City of Industry, CA, USA).

### Necromass incubation

Our study focused on characterizing the microbial communities on the same incubated necromass as analyzed in Fernandez *et al.* (2019). Briefly, litter bags containing necromass of each type were incubated individually *c.* 5 cm deep into the sphagnum in both hummocks and hollows within three replicate plots in the treatment chambers (five temperature and two $CO_2$ treatment levels) for 3, 12 and 24 months ($n = 720$). The decomposition incubations were initiated on 1 June 2016 and harvested on 2 September 2016 (3 months), 7 June 2017 (12 months) and 5 June 2018 (24 months). Upon harvest, litter bags were immediately put into plastic ziptop bags that were placed on ice in a cooler and transported back to the laboratory within 24 h for processing. Incubated necromass was then placed in the drying oven set at 27°C until mass readings stabilized. Following drying, dry mass of the necromass was measured.

### Necromass chemical profiling

The initial melanin content of each necromass type was assessed using a quantitative colorimetric assay (Fernandez & Koide, 2014). The initial C and N content of each necromass type was determined using an elemental analyzer at the University of Minnesota. Fourier transform infrared (FTIR) spectroscopy was used to investigate the biochemical composition of the necromass following incubation. Two milligrams of each necromass type were individually ground until homogenous in an agate mortar and pestle with 100 mg KBr. Samples were then pressed into disks and transmission FTIR spectra were recorded using a Thermo Scientific Nicolet iS5 spectrometer with an iD1 Transmission accessory. Sixty-four scans were averaged across the 4000–400 $cm^{-1}$ range at a resolution of 4 $cm^{-1}$. Background subtraction was applied using a pure KBr spectrum, and a baseline correction was applied to remove baseline distortions. Both background subtraction and baseline correction were done in Omnic, v.9 (Thermo Fisher Scientific Inc., Waltham, MA, USA), while peak heights were normalized by calculating *z*-scores before final analysis. To link the treatment effects with residual necromass chemistry, peaks corresponding with chemical bonds in common organic polymers were identified (Supporting Information Table S1) and normalized peak height values were used in statistical analyses.

### Molecular analyses

Remaining necromass not used for the FTIR analyses from the 3- and 12-month incubations was subjected to bacterial and fungal community molecular identification. (A loss of replication from the 24-month incubation as a result of litter bag disappearances in multiple plots prevented a balanced sampling at this time period. As such, all 24-month samples were excluded from our community analyses.) In total, 160 samples were analyzed (four necromass types × five temperatures × two $CO_2$ concentrations × two microtopographies × two incubation times). Total genomic DNA was extracted with PowerSoil kits (MoBio, Carlsbad, CA, USA), with all of the remaining fungal material from each sample added to the kit lysis tubes. Before extraction, the necromass samples were bead-beaten (BioSpec Products, Bartlesville, OK, USA) for 5 s to ensure homogenization. The remainder of the extraction followed the manufacturer's instructions. A DNA extraction blank (lysis tubes with no substrate added) was also included. To study bacterial and fungal community composition, we amplified 16S rRNA and ITS2 regions using the following primer combinations: bacteria, 515F 5′-GTGCCAGCMGCCGCGGTAA-3′ and 806R 5′-GGACTACHVHHHTWTCTAAT-3′ (Caporaso *et al.*, 2012); and fungi, fITS7a 5′-GTGARTCATCGARTCTTTG-3′ and ITS4 5′-TCCTCCGCTTATTGATATGC-3′ (Ihrmark *et al.*, 2012). We used one-step PCR with tagged primers following protocols for PCR reaction, settings and library preparation steps described in Mundra *et al.* (2021). Molecular data was generated from two full Flow-Cell runs and Paired-End (PE: 2 × 300 bp) sequencing were performed with Illumina Miseq.

### Bioinformatics analyses

We followed a consistent bioinformatic analysis pipeline for both bacterial and fungal analyses as described previously (Mundra *et al.*, 2021). In brief, we used BayesHammer for error correction (Nikolenko *et al.*, 2013), Pear v.0.9.10 for reads merging (Zhang *et al.*, 2014), Fastx-Toolkit v.0.0.14 and Vsearch v.2.4.3 (Rognes *et al.*, 2016) for quality filtering, and Sdm v.1.41 (LotuS pipeline) for demultiplexing (Hildebrand *et al.*, 2014). Further, ITSx v.1.0.11 was used to extract the ITS region (Nilsson *et al.*, 2010) and reads with < 100 bp were excluded. Of a total of 10

and 21 million bacterial and fungal reads, 6.5 and 17.1 million remained after quality filtering. We used VSEARCH for dereplication, global singleton removal and sequence clustering at a 97% similarity threshold. Chimera analysis was conducted on the most common representative sequences using the '–uchime_denovo' algorithm (Edgar *et al.*, 2011), implemented in VSEARCH and operational taxonomic units (OTUs) with < 10 reads were removed. Taxonomic assignments for bacteria and fungi were performed using GREENGENE v.13.8 (DeSantis *et al.*, 2006; McDonald *et al.*, 2012) and UNITE v.6 (Kõljalg *et al.*, 2013) databases, respectively. From the bacterial dataset, we removed 27 OTUs identified as Archaea. For the fungal dataset, we excluded OTUs with no fungal taxonomic annotations (267), identified as protist (one), or having < 80% query coverage (30) and identity (one). To account for variation in total sequence read counts across samples, all analyses were based on counts rarefied to 2392 per sample and 35 000 per sample for the bacterial and the fungal datasets, respectively. Following quality filtering and rarefaction, 142 bacterial and 145 fungal samples were retained, representing a total of 339 664 and 5075 000 sequences belonging to 1505 bacterial and 689 fungal OTUs, respectively. Bacterial and fungal OTU tables are available in the Tables S2–S4.

Bacterial OTUs were assigned to copiotrophic and oligotrophic modes based on Trivedi *et al.* (2018). Specifically, all bacterial OTUs belonging to the phylum Bacteroidetes and classes alpha-Proteobacteria, beta-Proteobacteria and gamma-Proteobacteria were defined as copiotrophs, while bacterial OTUs belonging to the phylum Acidobacteria and class delta-Proteobacteria were defined as oligotrophs. Based on their assigned taxonomy, fungal OTUs were designated as having saprotrophic, pathogenic or symbiotrophic trophic modes using FUNGuild (Nguyen *et al.*, 2016). The symbiotrophic trophic mode was composed of root-associated fungi (i.e. endophytic, ericoid mycorrhizal and ectomycorrhizal fungi), with all of the lichenized fungi excluded from further analyses.

### Data analyses

Statistical analyses and data visualizations were performed using R (R Core Team, 2016) and considered significant at $P \leq 0.05$. Although the mass remaining for each of the four fungal necromass types was largely the same between the 3 and 12 month incubation times (Fernandez *et al.*, 2019), we analyzed the microbial community analyses at each incubation time separately to better understand the community patterns within each time period. In general, the microbial communities showed similar responses at 3 and 12 months, with some notable exceptions discussed later. To enhance the clarity of the overall results, the figures and table in the main text focus on the 3 month incubation time analyses, with all of the corresponding 12 month incubation time analyses provided in the Supporting Information (Tables S5–S7; Figs S1–S11). Bacterial and fungal OTU richness per sample was calculated in the VEGAN package (Oksanen *et al.*, 2013). To determine the independent and interactive effects of temperature (+ 0, + 2.25, + 4.5, + 6.75 and + 9°C), microtopography (hollow and hummock) and necromass type (*C. geophilum*, *M. bicolor*, *O. griseum* and *S. grisellus*) on bacterial and fungal OTU composition, a series of permutational multivariate analyses of variance (Anderson, 2001) were applied using the 'adonis' function in the VEGAN package. We choose to focus on these three treatments and their interactions and not to test for any $CO_2$ effect because we previously found that the $CO_2$ treatment had no significant effect on necromass mass loss (Fernandez *et al.*, 2019). Compositional variation among samples based on bacterial and fungal OTUs was visualized with nonmetric multidimensional scaling (NMDS) plots based on Bray–Curtis dissimilarity matrices. To examine the change in community composition between microtopographies associated with warming (e.g. whether hollow communities were becoming more like hummock communities or vice versa), we specifically compared the similarity of the bacterial and fungal communities in each warmed treatment (+ 2.25, + 4.5, + 6.75 and + 9°C) with those in each unwarmed treatment, using both hummock and hollow as reference + 0°C treatment. The 'envfit' function in the VEGAN package (Oksanen *et al.*, 2013) was used to test for relationships between the bacterial and fungal OTU composition and initial and final necromass chemical parameters. The effects of temperature on bacterial and fungal OTU richness and functional guild relative abundances were evaluated using one-way analysis of variance (ANOVA) for each microtopography independently (hollow and hummock). Additionally, temperature–guild abundance relationships were tested using Pearson's correlations for each microtopography. A one-way ANOVA was also used to test the effect of necromass type on the relative abundances of the fungal genera colonizing the incubated necromass. Before the ANOVAs, variance homoscedasticities were tested using Cochran's test and data were log-transformed if necessary. All higher abundance bacterial and fungal OTUs (representing a cumulative sum of 70% and 90% of relative abundances, respectively) were evaluated for significant association with necromass type using the INDICSPECIES package (De Caceres & Legendre, 2009). Only the significant indicator OTUs are presented ($P \leq 0.05$).

## Results

### Microbial community responses to temperature

Bacterial and fungal OTU richness on decaying necromass were comparable in hummocks and hollows in the + 0°C treatment (bacterial OTUs: hummock = 182 ± 25 and hollow = 183 ± 29; fungal OTUs: hummock = 153 ± 7 OTUs and hollow = 142 ± 10) (Fig. S12). Increasing temperature had no significant effect on bacterial or fungal OTU richness in hummocks (bacteria: $F_{4,28} = 0.32$, $P = 0.86$; fungi: $F_{4,30} = 1.35$, $P = 0.27$) or in hollows (bacteria: $F_{4,33} = 2.33$, $P = 0.07$; fungi: $F_{4,34} = 0.26$, $P = 0.90$ (Fig. S12)).

The composition of both bacterial and fungal OTU communities on decaying necromass was significantly influenced by temperature, microtopography and their interaction (Table 1; Fig. S2). Bacterial and fungal communities became significantly more similar between hummocks and hollows with increasing temperature (Fig. 1a,b). Using the + 0°C treatments as a

**Table 1** Permutational multivariate analyses of variance (*, $P \leq 0.05$; **, $P \leq 0.01$; ***, $P \leq 0.001$) of bacterial and fungal operational taxonomic unit (OTU) composition depending on temperature (+ 0, + 2.25, + 4.5, + 6.75 and + 9°C), microtopography (hollow and hummock), and necromass type (*Cenococcum geophilum*, *Meliniomyces bicolor*, *Oidiodendron griseum* and *Suillus grisellus*) based on Bray–Curtis dissimilarity following 3 months of field incubation.

| | Bacterial OTU composition | | | | | Fungal OTU composition | | | | |
|---|---|---|---|---|---|---|---|---|---|---|
| | df | *F* | $R^2$ | *P* | | df | *F* | $R^2$ | *P* | |
| **Temperature** | **4** | **1.97119** | **0.10640** | **0.001*** ** | **Temperature** | **4** | **2.2073** | **0.10331** | **0.001*** ** |
| **Microtopography** | **1** | **1.93165** | **0.02607** | **0.004** ** | **Microtopography** | **1** | **2.0064** | **0.02348** | **0.006** ** |
| **Necromass type** | **3** | **1.60256** | **0.06488** | **0.006** ** | **Necromass type** | **3** | **3.8959** | **0.13676** | **0.001*** ** |
| **Temperature × microtopography** | **4** | **1.43052** | **0.07721** | **0.011*** | **Temperature × microtopography** | **4** | **1.8586** | **0.08699** | **0.001*** ** |
| Temperature × necromass type | 12 | 0.85422 | 0.13832 | 0.947 | Temperature × necromass type | 12 | 0.7290 | 0.10235 | 1.000 |
| Microtopography × necromass type | 3 | 0.79518 | 0.03219 | 0.882 | Microtopography × necromass type | 3 | 0.8692 | 0.03051 | 0.779 |
| Temperature × microtopography × necromass type | 11 | 0.82940 | 0.12311 | 0.960 | Temperature × microtopography × necromass type | 11 | 0.8319 | 0.10707 | 0.965 |
| Residuals | 32 | 0.43182 | | | Residuals | 35 | 0.40953 | | |
| Total | 70 | | | | Total | 73 | | | |

Bold values highlight a significant treatment effect.

reference, the necromass-associated microbial communities in the warmed hollows became more similar to the reference hummock community (Fig. 1c,d), whereas the necromass-associated microbial communities in the warmed hummocks did not become more similar to the hollow reference (+ 0°C).

From a functional perspective, copiotrophic bacteria dominated the hummock (62% ± 7%), while hollow communities were more evenly distributed between copiotrophic (32% ± 10%) and oligotrophic bacteria (36% ± 12%) (Figs 2, S13). Both copiotrophic ($F_{4,33} = 5.21$, $P \leq 0.01$) and oligotrophic ($F_{4,33} = 6.97$, $P \leq 0.001$) bacterial abundances were significantly affected by the temperature treatments in the hollow (Table S5). By contrast, temperature had no significant effect on hummock-associated bacterial trophic groups. When analyzed as a continuous variable, temperature was significantly positively correlated with copiotrophic bacterial abundances and negatively with oligotrophic bacterial abundances in the hollows.

In the + 0°C treatment, saprotrophic (38 ± 11%), pathogenic (20 ± 12%), and symbiotrophic fungi (18 ± 8%) colonized fungal necromass incubated in the hummocks relatively evenly. By contrast, fungal saprotrophs (69 ± 15%) largely dominated in the hollows (Figs 2, S13). Increases in temperature in the hummocks were significantly associated with an increase in the relative abundances of saprotrophic fungi. In the hollows, increases in temperature correlated positively with the relative abundances of symbiotrophic fungi.

## Microbial community responses to necromass type

The composition of bacterial and fungal communities was also significantly influenced by necromass type (Table 1). Both bacterial composition and fungal composition were similar for three necromass types (*C. geophilum*, *O. griseum* and *S. grisellus*), but different on *M. bicolor* necromass (Fig. 3). These compositional differences were related to the initial necromass C (bacteria, $P \leq 0.05$; fungi, $P \leq 0.01$) and N content (bacteria, $P \leq 0.05$; fungi, $P \leq 0.05$) as well as the final $Aliphatics_{2924}$ (bacteria, $P \leq 0.01$; fungi, $P \leq 0.01$) and $Aliphatics_{2850}$ FTIR peaks (bacteria, $P \leq 0.01$; fungi, $P \leq 0.01$) (Table S7). Bacterial OTU composition was also significantly positively correlated, albeit to a lesser extent ($P \leq 0.05$), with one aromatics FTIR peak ($Aromatics_{840}$).

The bacterial community consisted primarily of alpha-, beta- and gamma-Proteobacteria, Sphingobacteria, Actinobacteria and Acidobacteria (Fig. S7). Alphaproteobacteria ($F_{3,67} = 4.44$, $P \leq 0.01$) and Spartobacteria ($F_{3,67} = 3.22$, $P \leq 0.05$) were less abundant on *M. bicolor* necromass. Among the 67 most abundant bacterial OTUs (i.e. those representing a total of 70% of the sequences), 10 were significant indicators of one necromass type based on INDICSPECIES analysis (Fig. S8): Comamonadaceae (OTU48) was an indicator of *C. geophilum* necromass; *Acidicapsa* (OTU103) and *Granulicella* (OTU80) were indicators of *M. bicolor* necromass; *Mycobacterium* (OTU7 and OTU839) and *Opitutus* (OTU11 and OTU51) were indicators of *O. griseum* necromass; and *Mucilaginibacter* (OTU19), *Labrys* (OTU58), *Rhizobium* (OTU29) and Verrucomicrobia (OTU77) were indicators of *S. grisellus* necromass.

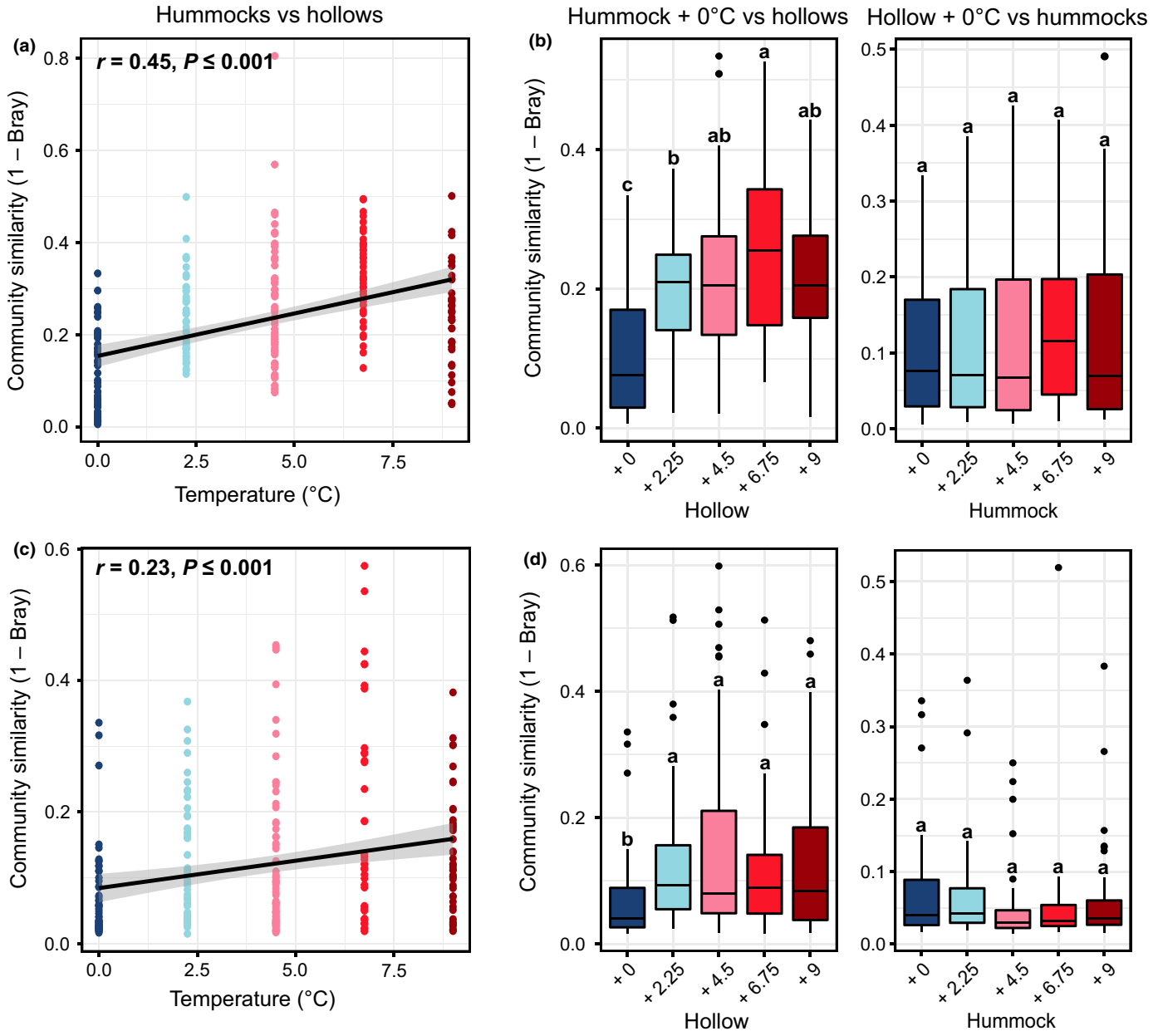


**Fig. 1** Similarity (1 – Bray–Curtis dissimilarity) of bacterial (a) and fungal (c) operational taxonomic unit (OTU) composition in hummocks and hollows in each of the five temperature treatments (+ 0, + 2.25, + 4.5, + 6.75 and + 9°C) following 3 months of field incubation. Gray shading represents the 95% confidence interval. Similarity of bacterial (b) and fungal (d) OTU composition in each temperature treatment compared with the unwarmed (+ 0) hummock and unwarmed (+ 0) hollow, respectively. Different letters indicate significant differences (Tukey's honestly significant difference, $P \leq 0.05$). Boxes correspond to median (line in box), 25$^{th}$ percentile (lower line) and 75$^{th}$ percentile (upper line) ranges. Whiskers extend from 25$^{th}$ and 75$^{th}$ percentile limits to the smallest and largest values that do not exceed 1.5 × interquartile range limit in each direction. Data beyond the end of the whiskers are plotted individually as circles.

The fungal community was dominated by the classes Leotiomycetes, Sordariomycetes, Eurotiomycetes and Agaricomycetes as well as subphyla Mucoromycotina and Mortierellomycotina (Fig. S9). Unlike the other necromass types, *M. bicolor* necromass was significantly enriched in fungi in the Eurotiomycetes ($F_{3,70} = 14.45$, $P \leq 0.001$) and depleted in those in the Agaricomycetes ($F_{3,70} = 4.27$, $P \leq 0.01$). Among the 56 most abundant fungal OTUs (i.e. those representing 90% of the sequences), 10 were significant indicators of one necromass type (Fig. S10). For those with taxonomic identification at the species level, *Lecanicillium fungicola* (OTU20) and *Meliniomyces variabilis* (OTU36) were indicators of *C. geophilum* necromass, *Oidiondendron maius* (OTU24), *Cadophora finlandica* (OTU22), *Talaromyces stollii* (OTU4), *Talaromyces proteolyticus* (OTU13) and *Meliniomyces variabilis* (OTU15, OTU45 and OTU2369) of *M. bicolor* necromass, *Oidiodendron pilicola* (OTU1) and *Mortierella macrocystis* (OTU 26) of *O. griseum* necromass, and *Trichoderma appalachiense* (OTU3) of *S. grisellus* necromass (Fig. 4).

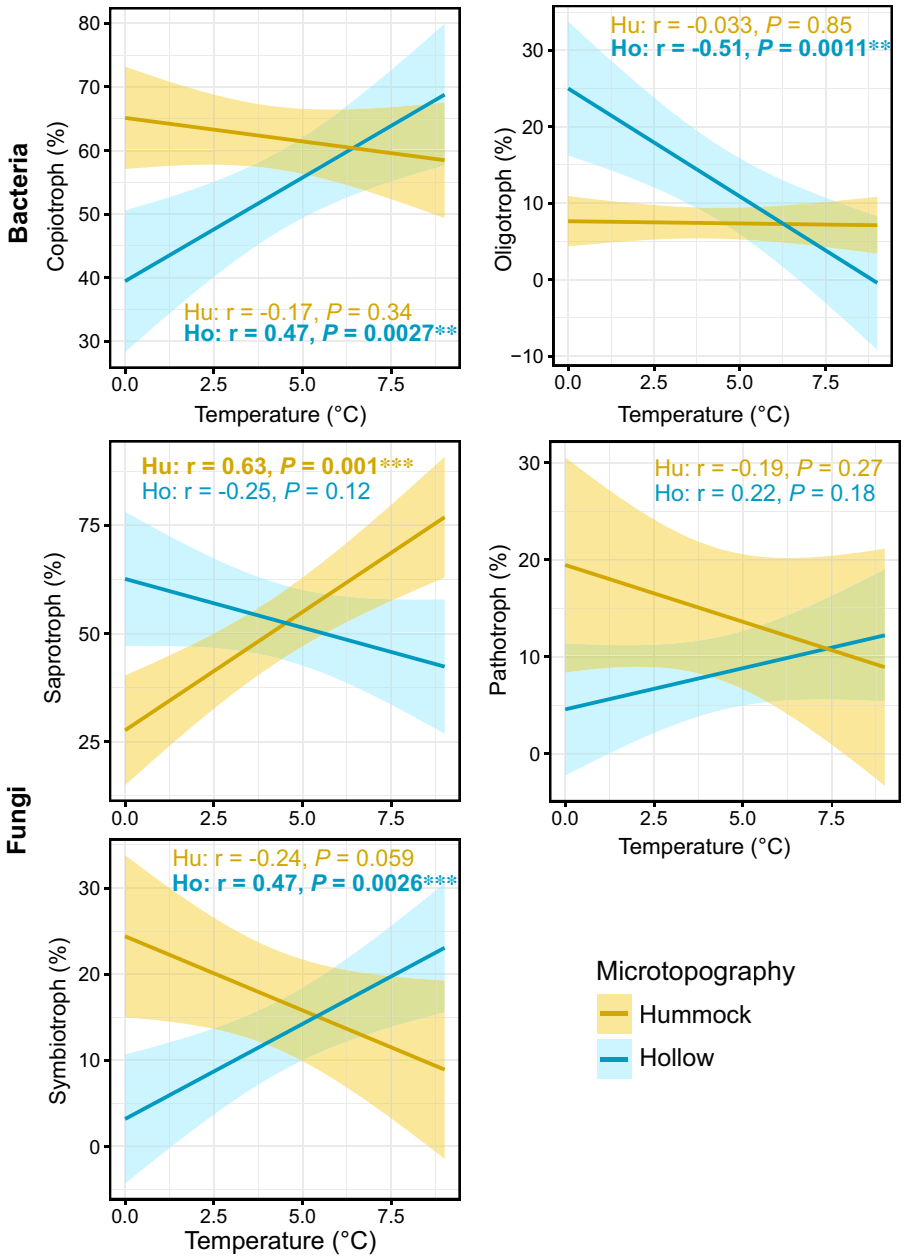


**Fig. 2** Relationships between bacterial and fungal functional guild relative abundances and temperature treatments depending on microtopography (Hu, hummock; Ho, hollow) following 3 months of field incubation (*, $P \leq 0.05$; **, $P \leq 0.01$; ***, $P \leq 0.001$). Shading represents the 95% confidence interval.

### Fungal genus-level response to necromass type

Colonizing fungi from the same genus as the incubated necromass were detected for three of the four genera. Specifically, *Meliniomyces*, *Oidiodendron* and *Suillus* were detected on all four necromass types, while the genus *Cenococcum* was not identified on any necromass type (Fig. 4). On average, OTUs in the genus *Suillus* showed no preference across necromass types, with relative abundances ranging from 0.47% on *S. grisellus* necromass to 1.51% on *C. geophilum* necromass ($F_{3,70} = 0.47$, $P = 0.70$). By contrast, necromass type significantly affected the relative abundances of *Meliniomyces* ($F_{3,70} = 5.06$, $P \leq 0.01$) and *Oidiodendron* OTUs ($F_{3,70} = 39.2$, $P \leq 0.001$), with both being highly enriched on necromass from the same genus (*M. bicolor* and *O. griseum*, respectively).

## Discussion

This study represents the first to examine the responses of microbial communities associated with decomposing mycorrhizal fungal necromass under manipulated environmental conditions. The warming treatments in the SPRUCE experiment have modified the abiotic conditions in the hummocks and hollows, with the hollows becoming less water-saturated (Fernandez *et al.*, 2019). Previously, we found that this change strongly influenced the rate at which mycorrhizal necromass decomposed (Fernandez *et al.*, 2019) and here we show that there were also significant shifts in microbial communities in the decomposing necromass, which were associated with temperature and microtopography. Specifically, we found that across necromass types, both bacterial and fungal communities in hollows became increasingly similar to

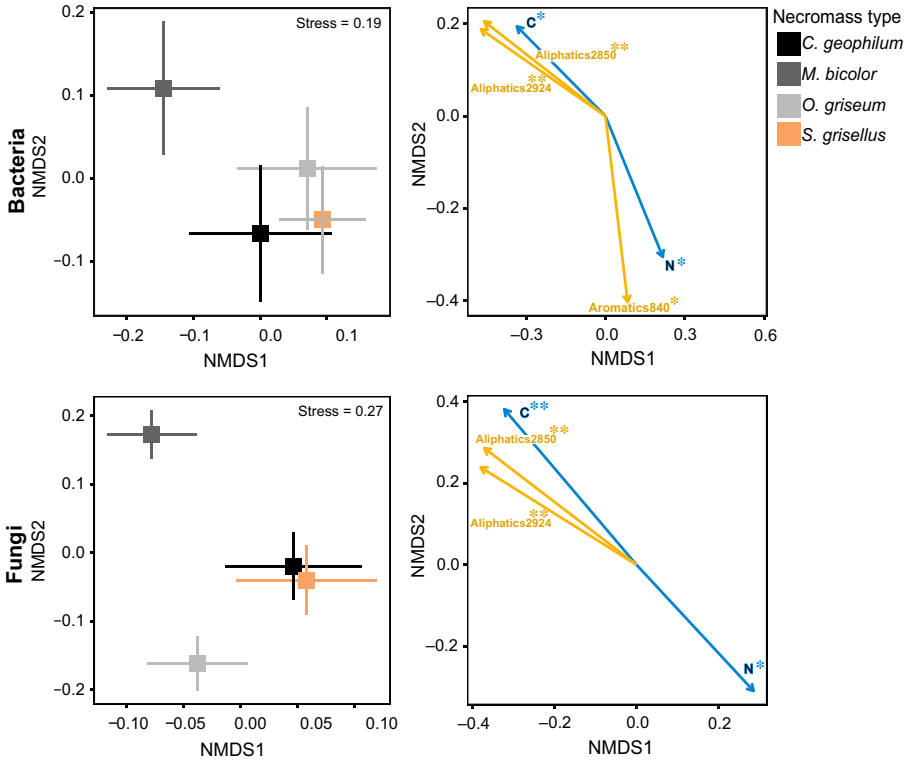


**Fig. 3** Nonmetric multidimensional scaling (NMDS) plots of bacterial and fungal operational taxonomic unit (OTU) composition depending on necromass type (*Cenococcum geophilum*, *Meliniomyces bicolor*, *Oidiodendron griseum* and *Suillus grisellus*) following 3 months of field incubation. Squares represent centroids, with lines representing 1 SE. Arrows represent vectors of necromass chemical parameters correlated with differences in community composition. Only the significant vectors are represented (*, $P \leq 0.05$; **, $P \leq 0.01$; ***, $P \leq 0.001$). Blue and yellow vectors represent initial and final necromass chemical parameters, respectively.

those in hummocks with increasing warming, a phenomenon we refer to as 'hummockification'. This trend was most strong after 3 months, whereas after 12 months this response was no longer present for the bacteria (because the community had already been 'hummockified'), but remained for the fungi (Fig. S4). Major structural shifts in fungal community structure with comparable warming were also observed in bulk peat soils by Asemaninejad *et al.* (2018) in a mesocosm experiment. Collectively, these results from different study systems and sample types suggest that the temperature-related trend we observed on mycorrhizal fungal necromass may be broadly representative of alterations in the microbial community present in warming peatlands, although the rapid turnover of fungal necromass relative to other organic matter substrates may make this microbial community particularly sensitive to altered environmental conditions.

With regard to our first research question, we found a strong correspondence between the effect of warming on mycorrhizal fungal necromass mass loss and microbial community composition; in both cases the changes as a result of warming were most pronounced in the hollows. Importantly, the observed changes in taxonomic composition appear to have notable functional consequences, given the shift from oligotrophic to copiotrophic bacterial dominance with increasing temperature in hollows (but not hummocks). This transition suggests that as temperatures increase, the capacity of bacterial communities to decompose complex substrates may be declining. The abundance trends also further reiterate the 'hummockification' pattern noted earlier, with both the bacterial copiotroph and oligotroph abundances in the hollows becoming increasingly similar to those in the hummocks as temperatures increase. Similar functional shifts were

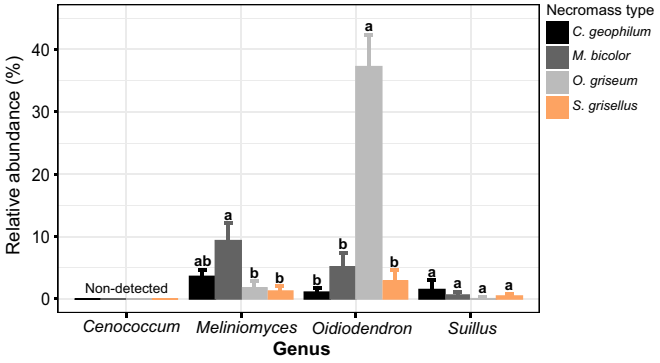


**Fig. 4** The relative abundance of *Cenococcum*, *Meliniomyces*, *Oidiodendron* and *Suillus* fungal genera depending on necromass type following 3 months of field incubation (*C. geophilum*, *M. bicolor*, *O. griseum* and *S. grisellus*) (± SE). Different letters indicate significant differences (Tukey's honestly significant difference, $P \leq 0.05$).

also observed in the fungal communities associated with the decomposing necromass, most notably a significant rise in the relative abundances of symbiotrophic fungi with increasing temperature in the hollows. While the specific consequences of these compositional changes are not yet clear, it is possible that they may lead to major modifications of the N cycle in the hollows through enhanced competition for nutrients with saprotrophic fungi (Fernandez & Kennedy, 2016).

Regarding our second question, the analysis of correlations between microbial community composition and chemical attributes of fungal necromass revealed similarities between and differences from previous observations. Here, we only analyzed the microbial communities in the later stages of decomposition

when the large majority of mass loss had already occurred (Fernandez *et al.*, 2019). Despite that, we found that initial necromass C and N content remained important predictors of the bacterial and fungal communities, which is similar to results found in other studies over shorter timescales (Brabcová *et al.*, 2018; Ryan *et al.*, 2020). The differences in decomposer community composition appeared to be largely associated with the unique chemistry of *Meliniomyces bicolor*, which has a much higher C : N ratio than the other three necromass types. More closely analyzing the chemistry of the remaining necromass, it appears that differences in aliphatic content, in particular (which was higher in *M. bicolor* necromass), were most strongly associated with variation in microbial community structure. We suspect that this pattern is probably a result of aliphatic compounds being an active target of catabolism once more labile substrates have been consumed. Interestingly, while in a previous study we found that initial melanin content was the strongest predictor of the amount of necromass remaining in this experiment study (Fernandez *et al.*, 2019), it was not a factor explaining significant differences in microbial community structure among the four necromass types. This result differs from results found in other systems (Fernandez & Kennedy, 2018), suggesting that more research is needed to better understand how different microbes process fungal melanin during necromass decomposition.

In relation to our third research question, we found a disproportionate amount of colonization of *Meliniomyces* and *Oidiodendron* fungal necromass by fungi from the same genera, but from different species than the ones used to generate necromass. To our knowledge, this differs from all previous necromass decomposition experiments where the dominant fungal OTUs came from taxa not related to the decomposing necromass (Drigo *et al.*, 2012; Brabcová *et al.*, 2016, 2018; Fernandez & Kennedy, 2018; Beidler *et al.*, 2020; Maillard *et al.*, 2020). If this taxon-specific response were something uniquely caused by the abiotic conditions in peatlands, we would have expected to see similar enrichment patterns on the other two necromass types, but that was not the case. Instead, it appears that taxa belonging to potential ericoid mycorrhizal genera have an enhanced capacity to colonize their congeneric necromass. The fact that potential ericoid mycorrhizal fungi are efficient colonizers of dead mycelium is consistent with a number of experimental studies that have demonstrated that ericoid mycorrhizal fungi are able to directly target chitin for decomposition and that much of the N present in necromass is transferred to the host plant (Leake & Read, 1990; Kerley & Read, 1995, 1998). Differences in chitin utilization between ericoid and ectomycorrhizal fungi were also demonstrated by Kerley & Read (1998), with ericoid mycorrhizal fungi having significantly higher growth on chitin than ectomycorrhizal fungal species (both related to *Suillus*). However, the high fungal cell wall decomposition abilities of the ericoid mycorrhizal fungi do not explain why they were extremely efficient at colonizing congeneric fungal necromass in our study. The mechanisms underpinning selective colonization of necromass from related species by the ericoid mycorrhizal fungi might be related to better detection of necromass hotspots in soil (chemotaxis) or some enzymatic advantages by comparison with phylogenetically distant fungal decomposers. Intriguingly, this potential enhanced capacity of ericoid mycorrhizal fungi to obtain N from necromass of phylogenetically related species may also help to explain the significantly improved performance of ericaceous shrubs in response to warming in the SPRUCE experiment and elsewhere (Malhotra *et al.*, 2020).

While this study provides a number of new insights into the ecological factors structuring necromass-associated microbial communities, there are important caveats that should be considered. The use of sequence reads as proxies for microbial abundances should always be interpreted with some caution owing to differences among taxa in gene copy numbers (Lofgren *et al.*, 2019), primer affinities (Taylor *et al.*, 2016) and amplicon lengths (Nguyen *et al.*, 2016). As such, future studies using non-molecular methods to assess taxon-specific abundances, such as phospholipid fatty acid analysis, will be important in validating the observed patterns. Our functional inferences also rely on accurate assignment based on existing databases. This can be particularly challenging for ericoid mycorrhizal fungi as a result of some taxa having mixed ecological strategies (e.g. *Meliniomyces* can form both ectomycorrhizal and ericoid mycorrhizas and *Oidiodendron* can present either symbiotrophic or saprotrophic trophic modes (Vrålstad *et al.*, 2002)). As such, we chose to analyze all root-associated fungal taxa by trophic mode rather than specific guild. Although there may be some concern about the initial drying temperature being sufficient to kill the four mycorrhizal fungi used in our incubations, had there been survival we would have expected some mass gain in the bags over time, which we did not observe. Further, we would also have expected to find the exact same four fungal taxa in the microbial communities on each type of decomposing necromass, which we did not. Together these results suggest there was no revival of the original substrate during the incubations. Lastly, we recognize that our litter-bag technique excludes potentially important decomposers, including soil fauna as well as roots (Crowther *et al.*, 2013; Brzostek *et al.*, 2015; Bradford *et al.*, 2016), which may alter microbial decomposer community composition in important ways (Maillard *et al.*, 2021).

Overall, our results indicate that warming in peatlands is likely to have significant consequences on the turnover of mycorrhizal fungal mycelium linked to shifts in microbial decomposer community composition. Specifically, the hollow microsites are likely to experience enhanced organic matter decomposition, as microbial communities adapted to the abiotic conditions in hummocks move deeper into the peat with water table decline. However, because warming can create more stressful conditions in hummocks (as a result of enhanced desiccation (Norby *et al.*, 2019)), it will be important to continue to track how the rooting depths of both trees and ericaceous shrubs respond to temperature changes (Malhotra *et al.*, 2020), as that will strongly affect where the majority of mycorrhizal fungal biomass grows and dies. Finally, a congeneric necromass colonization advantage might represent a new functional trait of the ericoid mycorrhizal fungi potentially involved in host plant nutrition in peatlands and deserves further field-based investigation.

## Acknowledgements

We would like to thank B. Lindahl and two anonymous reviewers for their helpful comments and suggestions on previous versions of this manuscript. Research was supported in part by a grant to PGK and HK from the Norwegian Centennial Chairs Program and the National Science Foundation (2038293 to PGK). The SPRUCE project is generously supported by U.S. Department of Energy, Office of Science, Biological and Environmental Research Program. The authors declare there are no conflict of interests.

## Author contributions

PGK and CWF designed the experiment. FM, CWF, SM, KAH, RKK, HK and PGK performed the experiment or collected, analyzed and interpreted the data. FM and PFK wrote the first draft of the manuscript. All the authors contributed to the final version of the manuscript.

## ORCID

Christopher W. Fernandez https://orcid.org/0000-0002-6310-6027
Katherine A. Heckman https://orcid.org/0000-0003-2265-4542
François Maillard https://orcid.org/0000-0002-2144-5629
Sunil Mundra https://orcid.org/0000-0002-0535-118X

## Data availability

Bacterial and fungal rarefied OTU tables and their associated mapping files are included in the Supporting Information. Other data regarding fungal necromass mass losses and chemical parameters that support the findings of this study are available on request from the corresponding author.

## References

**Akroume E, Maillard F, Bach C, Hossann C, Brechet C, Angeli N, Zeller B, Saint-André L, Buée M. 2019.** First evidences that the ectomycorrhizal fungus *Paxillus involutus* mobilizes nitrogen and carbon from saprotrophic fungus necromass. *Environmental Microbiology* **21**: 197–208.

**Andersen R, Chapman SJ, Artz RRE. 2013.** Microbial communities in natural and disturbed peatlands: a review. *Soil Biology and Biochemistry* **57**: 979–994.

**Anderson MJ. 2001.** A new method for non-parametric multivariate analysis of variance. *Austral Ecology* **26**: 32–46.

**Asemaninejad A, Thorn RG, Branfireun BA, Lindo Z. 2018.** Climate change favours specific fungal communities in boreal peatlands. *Soil Biology and Biochemistry* **120**: 28–36.

**Asemaninejad A, Thorn RG, Branfireun BA, Lindo Z. 2019.** Vertical stratification of peatland microbial communities follows a gradient of functional types across hummock–hollow microtopographies. *Ecoscience* **26**: 249–258.

**Asemaninejad A, Thorn RG, Lindo Z. 2017.** Vertical distribution of fungi in hollows and hummocks of boreal peatlands. *Fungal Ecology* **27**: 59–68.

**Beidler KV, Phillips RP, Andrews E, Maillard F, Mushinski RM, Kennedy PG. 2020.** Substrate quality drives fungal necromass decay and decomposer community structure under contrasting vegetation types. *Journal of Ecology* **108**: 1845–1859.

**Belyea LR, Malmer N. 2004.** Carbon sequestration in peatland: patterns and mechanisms of response to climate change. *Global Change Biology* **10**: 1043–1052.

**Brabcová V, Nováková M, Davidová A, Baldrian P. 2016.** Dead fungal mycelium in forest soil represents a decomposition hotspot and a habitat for a specific microbial community. *New Phytologist* **210**: 1369–1381.

**Brabcová V, Štursová M, Baldrian P. 2018.** Nutrient content affects the turnover of fungal biomass in forest topsoil and the composition of associated microbial communities. *Soil Biology and Biochemistry* **118**: 187–198.

**Bradford MA, Berg B, Maynard DS, Wieder WR, Wood SA. 2016.** Understanding the dominant controls on litter decomposition. *Journal of Ecology* **104**: 229–238.

**Bragazza L, Parisod J, Buttler A, Bardgett RD. 2013.** Biogeochemical plant–soil microbe feedback in response to climate warming in peatlands. *Nature Climate Change* **3**: 273–277.

**Breeuwer A, Robroek BJ, Limpens J, Heijmans MM, Schouten MG, Berendse F. 2009.** Decreased summer water table depth affects peatland vegetation. *Basic and Applied Ecology* **10**: 330–339.

**Brzostek ER, Dragoni D, Brown ZA, Phillips RP. 2015.** Mycorrhizal type determines the magnitude and direction of root-induced changes in decomposition in a temperate forest. *New Phytologist* **206**: 1274–1282.

**Caporaso JG, Lauber CL, Walters WA, Berg-Lyons D, Huntley J, Fierer N, Owens SM, Betley J, Fraser L, Bauer M *et al.* 2012.** Ultra-high-throughput microbial community analysis on the Illumina HiSeq and MiSeq platforms. *ISME Journal* **6**: 1621–1624.

**Clemmensen KE, Finlay RD, Dahlberg A, Stenlid J, Wardle DA, Lindahl BD. 2015.** Carbon sequestration is related to mycorrhizal fungal community shifts during long-term succession in boreal forests. *New Phytologist* **205**: 1525–1536.

**Crowther TW, Stanton DWG, Thomas SM, A'Bear AD, Hiscox J, Jones TH, Voriskova J, Baldrian P, Boddy L. 2013.** Top-down control of soil fungal community composition by a globally distributed keystone consumer. *Ecology* **94**: 2518–2528.

**De Caceres M, Legendre P. 2009.** Associations between species and groups of sites: indices and statistical inference. *Ecology* **90**: 3566–3574.

**DeSantis TZ, Hugenholtz P, Larsen N, Rojas M, Brodie EL, Keller K, Huber T, Dalevi D, Hu P, Andersen GL. 2006.** Greengenes, a chimera-checked 16S rRNA gene database and workbench compatible with ARB. *Applied and Environment Microbiology* **72**: 5069–5072.

**Drigo B, Anderson IC, Kannangara GSK, Cairney JWG, Johnson D. 2012.** Rapid incorporation of carbon from ectomycorrhizal mycelial necromass into soil fungal communities. *Soil Biology and Biochemistry* **49**: 4–19.

**Edgar RC, Haas BJ, Clemente JC, Quince C, Knight R. 2011.** UCHIME improves sensitivity and speed of chimera detection. *Bioinformatics* **27**: 2194–2200.

**Fehrer J, Réblová M, Bambasová V, Vohník M. 2019.** The root-symbiotic *Rhizoscyphus ericae* aggregate and *Hyaloscypha* (Leotiomycetes) are congeneric: phylogenetic and experimental evidence. *Studies in Mycology* **92**: 195–225.

**Fernandez CW, Heckman K, Kolka R, Kennedy PG. 2019.** Melanin mitigates the accelerated decay of mycorrhizal necromass with peatland warming. *Ecology Letters* **22**: 498–505.

**Fernandez CW, Kennedy PG. 2016.** Revisiting the 'Gadgil effect': do interguild fungal interactions control carbon cycling in forest soils? *New Phytologist* **209**: 1382–1394.

**Fernandez CW, Kennedy PG. 2018.** Melanization of mycorrhizal fungal necromass structures microbial decomposer communities. *Journal of Ecology* **106**: 468–479.

**Fernandez CW, Koide RT. 2014.** Initial melanin and nitrogen concentrations control the decomposition of ectomycorrhizal fungal litter. *Soil Biology and Biochemistry* **77**: 150–157.

**Fernandez CW, Langley JA, Chapman S, McCormack ML, Koide RT. 2016.** The decomposition of ectomycorrhizal fungal necromass. *Soil Biology and Biochemistry* **93**: 38–49.

**Gallego-Sala AV, Charman DJ, Brewer S, Page SE, Prentice IC, Friedlingstein P, Moreton S, Amesbury MJ, Beilman DW, Björck S *et al.* 2018.** Latitudinal

limits to the predicted increase of the peatland carbon sink with warming. *Nature Climate Change* **8**: 907–913.

**García FC, Bestion E, Warfield R, Yvon-Durocher G. 2018.** Changes in temperature alter the relationship between biodiversity and ecosystem functioning. *Proceedings of the National Academy of Sciences, USA* **115**: 10989–10994.

**Gorham E. 1991.** Northern peatlands: role in the carbon cycle and probable responses to climatic warming. *Ecological Applications* **1**: 182–195.

**Hambleton S, Sigler L. 2005.** *Meliniomyces*, a new anamorph genus for root-associated fungi with phylogenetic affinities to *Rhizoscyphus ericae* (≡ *Hymenoscyphus ericae*), Leotiomycetes. *Studies in Mycology* **53**: 1–27.

**Hanson P, Phillips J, Norby R, Warren J, Griffiths N, Ricciuto D. 2019.** Peatland responses to warming and elevated $CO_2$: $CO_2$ and $CH_4$ flux responses, the status of vegetation net primary production and implications for ecosystem carbon exchange after 3-years of manipulation. *Geophysical Research Abstracts* **21**: Article ID: 11610.

**Hanson PJ, Riggs JS, Nettles WR IV, Phillips JR, Krassovski MB, Hook LA, Gu L, Richardson AD, Aubrecht DM, Ricciuto DM *et al.* 2017.** Attaining whole-ecosystem warming using air and deep-soil heating methods with an elevated $CO_2$ atmosphere. *Biogeosciences* **14**: 861–883.

**Hildebrand F, Tadeo R, Voigt AY, Bork P, Raes J. 2014.** LotuS: an efficient and user-friendly OTU processing pipeline. *Microbiome* **2**: 30.

**Ihrmark K, Bodeker ITM, Cruz-Martinez K, Friberg H, Kubartova A, Schenck J, Strid Y, Stenlid J, Brandstrom-Durling M, Clemmensen KE *et al.* 2012.** New primers to amplify the fungal ITS2 region—evaluation by 454-sequencing of artificial and natural communities. *FEMS Microbiology Ecology* **82**: 666–677.

**Ito A, Reyer CP, Gädeke A, Ciais P, Chang J, Chen M, François L, Forrest M, Hickler T, Ostberg S *et al.* 2020.** Pronounced and unavoidable impacts of low-end global warming on northern high-latitude land ecosystems. *Environmental Research Letters* **15**: e044006.

**Kerley SJ, Read DJ. 1995.** The biology of mycorrhiza in the Ericaceae: XVIII. Chitin degradation by *Hymenoscyphus ericae* and transfer of chitin-nitrogen to the host plant. *New Phytologist* **131**: 369–375.

**Kerley SJ, Read DJ. 1998.** The biology of mycorrhiza in the Ericaceae. XX. Plant and mycorrhizal necromass as nitrogenous substrates for the ericoid mycorrhizal fungus *Hymenoscyphus ericae* and its host. *New Phytologist* **139**: 353–360.

**Kõljalg U, Nilsson RH, Abarenkov K, Tedersoo L, Taylor AFS, Bahram M, Bates ST, Bruns TD, Bengtsson-Palme J, Callaghan TM *et al.* 2013.** Towards a unified paradigm for sequence-based identification of fungi. *Molecular Ecology* **22**: 5271–5277.

**Leake JR, Read DJ. 1990.** Chitin as a nitrogen source for mycorrhizal fungi. *Mycological Research* **94**: 993–995.

**Lofgren LA, Uehling JK, Branco S, Bruns TD, Martin F, Kennedy PG. 2019.** Genome-based estimates of fungal rDNA copy number variation across phylogenetic scales and ecological life-styles. *Molecular Ecology* **28**: 721–730.

**Maillard F, Kennedy PG, Adamczyk B, Heinonsalo J, Buée M. 2021.** Root presence modifies the long-term decomposition dynamics of fungal necromass and the associated microbial communities in a boreal forest. *Molecular Ecology* **30**: 1921–1935.

**Maillard F, Schilling J, Andrews E, Schreiner KM, Kennedy P. 2020.** Functional convergence in the decomposition of fungal necromass in soil and wood. *FEMS Microbiology Ecology* **96**: fiz209.

**Malhotra A, Brice DJ, Childs J, Graham JD, Hobbie EA, Vander Stel H, Feron SC, Hanson PJ, Iversen CM. 2020.** Peatland warming strongly increases fine-root growth. *Proceedings of the National Academy of Sciences, USA* **117**: 17627–17634.

**McDonald D, Price MN, Goodrich J, Nawrocki EP, DeSantis TZ, Probst A, Andersen GL, Knight R, Hugenholtz P. 2012.** An improved Greengenes taxonomy with explicit ranks for ecological and evolutionary analyses of bacteria and archaea. *ISME Journal* **6**: 610–618.

**Moore T, Basiliko N. 2006.** Decomposition in boreal peatlands. In: *Boreal peatland ecosystems. Ecological studies (analysis and synthesis), vol 188.* Berlin, Heidelberg: Springer, 125–143.

**Moore TR, Bubier JL, Bledzki L. 2007.** Litter decomposition in temperate peatland ecosystems: the effect of substrate and site. *Ecosystems* **10**: 949–963.

**Moore TR, Dalva M. 1993.** The influence of temperature and water table position on carbon dioxide and methane emissions from laboratory columns of peatland soils. *Journal of Soil Science* **44**: 651–664.

**Mundra S, Kjønaas OJ, Morgado LN, Krabberød AK, Ransedokken Y, Kauserud H. 2021.** Soil depth matters: shift in composition and inter-kingdom co-occurrence patterns of microorganisms in forest soils. *FEMS Microbiology Ecology* **97**: fiab022.

**Nguyen NH, Song Z, Bates ST, Branco S, Tedersoo L, Menke J, Kennedy PG. 2016.** FUNGuild: an open annotation tool for parsing fungal community datasets by ecological guild. *Fungal Ecology* **20**: 241–248.

**Nikolenko SI, Korobeynikov AI, Alekseyev MA. 2013.** BayesHammer: Bayesian clustering for error correction in single-cell sequencing. *BMC Genomics* **14**: S7.

**Nilsson RH, Veldre V, Hartmann M, Unterseher M, Amend A, Bergsten J, Kristiansson K, Ryberg M, Jumpponen A, Abarenkov K. 2010.** An open source software package for automated extraction of ITS1 and ITS2 from fungal ITS sequences for use in high-throughput community assays and molecular ecology. *Fungal Ecology* **3**: 284–287.

**Norby RJ, Childs J, Hanson PJ, Warren JM. 2019.** Rapid loss of an ecosystem engineer: sphagnum decline in an experimentally warmed bog. *Ecology and Evolution* **9**: 12571–12585.

**Oksanen J, Blanchet FG, Kindt R, Legendre P, Minchin PR, O'Hara RB, Simpson GL, Solymos P, Stevens MHH, Szoecs E, Wagner E. 2013.** *VEGAN: community ecology package, v.2.0-7. R package.* [WWW document] URL http://CRAN.R-project.org/package=vegan.

**R Core Team. 2016.** *R: a language and environment for statistical computing.* Vienna, Austria: R Foundation for Statistical Computing. [WWW document] URL https://www.R-project.org/.

**Read DJ, Leake JR, Perez-Moreno J. 2004.** Mycorrhizal fungi as drivers of ecosystem processes in heathland and boreal forest biomes. *Canadian Journal of Botany* **82**: 1243–1263.

**Reich PB, Sendall KM, Rice K, Rich RL, Stefanski A, Hobbie SE, Montgomery RA. 2015.** Geographic range predicts photosynthetic and growth response to warming in co-occurring tree species. *Nature Climate Change* **5**: 148–152.

**Robroek BJ, Limpens J, Breeuwer A, Schouten MG. 2007.** Effects of water level and temperature on performance of four *Sphagnum* mosses. *Plant Ecology* **190**: 97–107.

**Rognes T, Flouri T, Nichols B, Quince C, Mahé F. 2016.** VSEARCH: a versatile open source tool for metagenomics. *PeerJ* **4**: e2584.

**Ryan ME, Schreiner KM, Swenson JT, Gagne J, Kennedy PG. 2020.** Rapid changes in the chemical composition of degrading ectomycorrhizal fungal necromass. *Fungal Ecology* **45**: 100922.

**Samson M, Słowińska S, Słowiński M, Lamentowicz M, Barabach J, Harenda K, Zielińska M, Robroek BJ, Jassey VE, Buttler A *et al.* 2018.** The impact of experimental temperature and water level manipulation on carbon dioxide release in a poor fen in Northern Poland. *Wetlands* **38**: 551–563.

**Sebestyen SD, Dorrance C, Olson DM, Verry ES, Kolka RK, Elling AE, Kyllander R. 2011.** Long-term monitoring sites and trends at the Marcell experimental forest. In: Kolka RK, Sebestyen SD, Verry ES, Brooks KN, eds. *Peatland biogeochemistry and watershed hydrology at the Marcell experimental forest.* Boca Raton, FL, USA: CRC Press, 15–71.

**Serreze MC, Walsh JE, Chapin FS III, Osterkamp T, Dyurgerov M, Romanovsky V, Oechel WC, Morison J, Zhang T, Barry RG. 2000.** Observational evidence of recent change in the northern high-latitude environment. *Climate Change* **46**: 159–207.

**Taylor DL, Walters WA, Lennon NJ, Bochicchio J, Krohn A, Caporaso JG, Pennanen T. 2016.** Accurate estimation of fungal diversity and abundance through improved lineage-specific primers optimized for Illumina amplicon sequencing. *Applied and Environmental Microbiology* **82**: 7217–7226.

**Traill LW, Lim ML, Sodhi NS, Bradshaw CJ. 2010.** Mechanisms driving change: altered species interactions and ecosystem function through global warming. *Journal of Animal Ecology* **79**: 937–947.

**Trivedi P, Wallenstein MD, Delgado-Baquerizo M, Singh BK. 2018.** Chapter 3 – microbial modulators and mechanisms of soil carbon storage. In: Singh BK, ed. *Soil carbon storage.* Cambridge, MA, USA: Academic Press, 73–115.

**Vrålstad T, Schumacher T, Taylor AF. 2002.** Mycorrhizal synthesis between fungal strains of the *Hymenoscyphus ericae* aggregate and potential ectomycorrhizal and ericoid hosts. *New Phytologist* **153**: 143–152.
**Wang M, Moore TR, Talbot J, Riley JL. 2015.** The stoichiometry of carbon and nutrients in peat formation. *Global Biogeochemical Cycles* **29**: 113–121.
**Zhang J, Kobert K, Flouri T, Stamatakis A. 2014.** PEAR: a fast and accurate illumina paired-end reAd mergeR. *Bioinformatics* **2014**: 614–620.
**Zhang Z, Phillips RP, Zhao W, Yuan Y, Liu Q, Yin H. 2019.** Mycelia-derived C contributes more to nitrogen cycling than root- derived C in ectomycorrhizal alpine forests. *Functional Ecology* **33**: 346–359.

## Supporting Information

Additional Supporting Information may be found online in the Supporting Information section at the end of the article.

**Fig. S1** Bacterial and fungal OTU richness depending on the temperature treatment separated by microtopography.

**Fig. S2** NMDS analysis of bacterial and fungal OTU composition depending on the temperature treatment and microtopography.

**Fig. S3** Similarity of bacterial and fungal OTU composition in hummocks and hollows.

**Fig. S4** Relative abundances of the bacterial and fungal trophic modes depending on the temperature treatment separated by microtopography.

**Fig. S5** Relationships between bacterial and fungal functional guild relative abundances and temperature treatments depending on microtopography.

**Fig. S6** NMDS analysis of bacterial and fungal OTU composition depending on necromass type.

**Fig. S7** Relative abundances of the most abundant bacterial classes depending on the necromass type.

**Fig. S8** Relative abundance of bacterial OTUs contributing to 70% of the total sequences depending on necromass.

**Fig. S9** Relative abundances of the most abundant fungal classes depending on the necromass type.

**Fig. S10** Relative abundance of fungal OTUs contributing to 90% of the total sequences depending on the necromass type.

**Fig. S11** Relative abundance of *Cenococcum*, *Meliniomyces*, *Oidiodendron* and *Suillus* fungal genera depending on the necromass type.

**Fig. S12** Bacterial and fungal OTU depending on the temperature treatment separated by microtopography.

**Fig. S13** Relative abundances of the bacterial and fungal trophic modes depending on the temperature treatment separated by microtopography.

**Table S1** FTIR spectra compound assignments.

**Table S2** Rarefied bacterial OTU table.

**Table S3** Rarefied fungal OTU table.

**Table S4** Mapping table for the bacterial and fungal OTU tables.

**Table S5** Effects of temperature on bacterial and fungal trophic mode relative abundances.

**Table S6** PERMANOVA analyses of bacterial and fungal OTU composition depending on temperature, microtopography and necromass type.

**Table S7** Envfit analysis testing for the relationships between necromass initial and final chemical parameters and the structure of the bacterial and fungal communities.

Please note: Wiley Blackwell are not responsible for the content or functionality of any Supporting Information supplied by the authors. Any queries (other than missing material) should be directed to the *New Phytologist* Central Office.